30th NENE 2021
September 6 - 9
BLED-SLOVENIA
International Conference Nuclear Energy for New Europe

Analysis Of The Effect Of Krško NPP Ex-Core Detector Position On Their Response

Tanja Goričanec[a], **Marjan Kromar**[a], **Andrej Kavčič**[b], **Bor Kos**[a],
Rok Bizjak[b], **Igor Lengar**[a], **Božidar Krajnc**[b], **Luka Snoj**[a]
[a] Reactor Physics Department, Jožef Stefan Institute
Jamova cesta 39
SI-1000 Ljubljana, Slovenia
[b] Krško Nuclear Power Plant
Vrbina 12
SI-8270 Krško, Slovenia
tanja.goricanec@ijs.si, marjan.kromar@ijs.si, andrej.kavcic@nek.si, bor.kos@ijs.si,
rok.bizjak@nek.si, igor.lengar@ijs.si, bozidar.krajnc@nek.si, luka.snoj@ijs.si

ABSTRACT

During an earthquake on the 29th of December 2020, the Krško NPP automatically shut down due to the trigger of the negative neutron flux rate signal on the power range nuclear instrumentation (PRNI). From the time course of the detector signal it can be concluded that there is a possibility that the fluctuation in the detector signal was caused by the mechanical movement of the ex-core neutron detectors or pressure vessel components, and not by the actual change in the reactor power. The aim of the analysis was to assess the difference in neutron flux at the ex-core detector position if the detector is moved for 5 cm in the radial or axial direction. In addition, the effect of core barrel movement for 5 mm in the radial direction was analysed. The analysis is supplemented with the thermal and total neutron flux gradient calculation in radial, axial and azimuthal directions. Monte Carlo particle transport code MCNP was used to study changes in the ex-core detector response for the above-mentioned scenarios. Power and intermediate-range detectors were analysed separately since they are constructed differently and exhibit different response characteristics. It was found that the power range ex-core detector movement has a negligible effect on the value of thermal neutron flux at the active part of the detector. However, the 5 cm radial movement of the intermediate-range detector leads to 7 % - 8 % change in thermal neutron flux within the active intermediate-range detector region. The analysis continued with the evaluation of the effect of core barrel movement on the ex-core detector response. It was determined that the 5 mm core barrel radial oscillation can lead to 9 % - 10 % change in thermal neutron flux within the active detector region. Analysis showed that the mechanical movement of ex-core neutron detectors could not explain the fluctuations in the ex-core detector signal. However, the core barrel oscillations could be a probable reason for the observed fluctuations in the ex-core detector signal during an earthquake.

1 INTRODUCTION

The ex-core detector system in Krško NPP monitors neutron flux from shutdown conditions to 120 % of full power. This represents ex-core neutron flux variations from 10^{-1}-10^{11}

n/(cm^2 s). To cover such a large flux range three types of neutron detectors are utilised for continuous power reading: source range nuclear instrumentation (SRNI), intermediate-range nuclear instrumentation (IRNI) and power range nuclear instrumentation (PRNI). For the power reading on the source range level (SRNI), the BF3 counters are used, while the compensated ionisation chambers are used for the power reading in the intermediate-range (IRNI). The SRNI and IRNI detectors are positioned inside the polyethylene cover, which slows down the fast neutrons coming from the reactor core to the thermal energies, which can be detected. During the normal power plant operation (at full power) the uncompensated ionisation chambers as power range detectors (PRNI) are used. The ex-core neutron detectors are position inside the wells next to the pressure vessel. PRNI are positioned in 4 symmetric locations around the reactor core, with two power range detectors per channel. Arrangement of ex-core neutron detectors around the Krško core is presented in Figure 1.

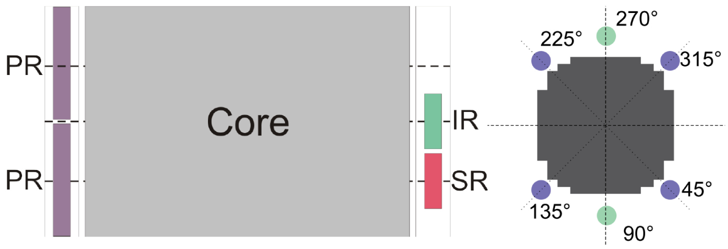

(a) Axial positions. (b) Azimuthal positions.

Figure 1: Schematic view of ex-core detector positions in Krško NPP. Source range (SR) detectors are presented in red, intermediate range (IR) detectors in green and power range (PR) detectors in purple.

2 COMPUTATIONAL MODEL

A computational model of the containment building, reactor pressure vessel, reactor core and ex-core detectors, used for presented calculations, was developed using Monte Carlo neutron transport code MCNP6.1.1. [1] with ENDF/B-VIII.0 nuclear data library [2]. The containment building computational model used in calculations is presented in Figure 2. Explicitly modelled ex-core detectors with the updated surrounding concrete shape used in calculations are presented in right hand side of figure in Figure 2. When studying their response, the polyethylene cover surrounding the IRNI has to be taken into account. The polyethylene cover slows down fast neutrons escaping reactor core to thermal energies, which can be detected. Unlike IRNI, PRNI is not covered with polyethylene. Therefore, IRNI detects approximately total neutron flux (ϕ_{tot}) at their position, while PRNI detects approximately thermal neutron flux (ϕ_{th}) at their position. The upper energy limits for neutron energy groups used in this paper are: 0.625 eV for thermal, 0.1 MeV for epithermal and 20 MeV for fast neutron flux.

To speed up the neutron transport from the reactor core to the ex-core neutron detectors, fixed neutron source was generated from the criticality calculation and weight windows were generated with the ADVANTG code version 3.2.1. [3]. Weight windows were generated using $bplus$ data library based on the ENDF/B-VII.0 nuclear data library and FW-CADIS methodology [3]. For other solver options default values were used. To ensure the final results are valid and converged, statistical tests were verified.

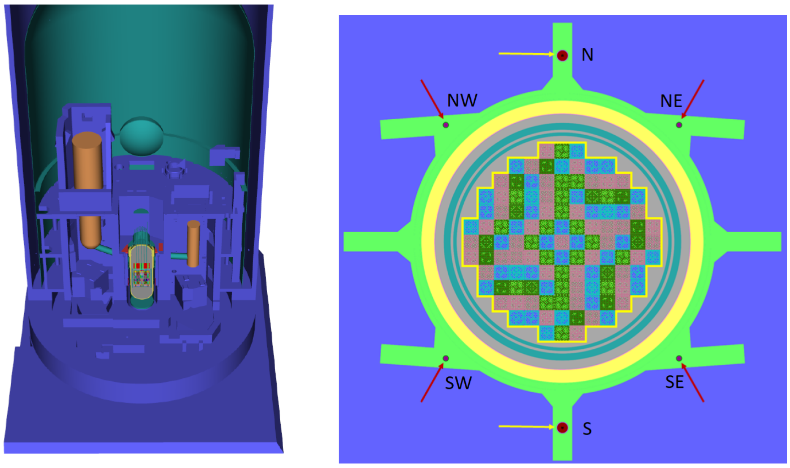

(a) Containment building.

(b) Detector locations (PRNI with red arrows and IRNI with yellow arrows) and surrounding concrete.

Figure 2: Schematic view of the MCNP model.

The hybrid code ADVANTG used to generate weight windows to speed up neutron transport outside the reactor core can not be used for eigenvalue problems. To use ADVANTG code, the core criticality calculation had to be translated to a fixed source model [4]. Different geometries and prompt fission neutron spectra for fixed source description were compared in previous research [5, 6], where the need for describing pin-wise neutron source with using prompt fission neutron spectra calculated from weighting prompt neutron fission spectra of important isotopes based on calculated reaction rates was identified. Fixed neutron source used for ex-core calculations presented in this paper was described with cylinders on fuel pin scale in 24 equally spaced axial layers. For calculations presented in this paper, fixed neutron source represented hot full power (HFP) core state for generic fuel cycle of Krško NPP (25^{th} fuel cycle) for the beginning of cycle (BOC) and end of cycle (EOC) state. BOC represents reactor core with 190 MWd/tU burnup and EOC with 17669 MWd/tU burnup. Calculations were performed for full reactor power of 1994 MW.

3 CALCULATION PROCEDURE

The calculation procedure designed to obtain ex-core detector response in a typical PWR NPP is schematically presented in Figure 3. Firstly, the deterministic code package CORD-2 [7] is used to obtain input parameters (temperatures, densities and isotopic compositions) for MCNP core model. All parameters are reported for individual fuel assembly in 10 axial layers, taking into account quadrant symmetry. In the next step, a subroutine McCord [8] is implemented to generate Monte Carlo neutron transport code MCNP [1] full core input from the CORD-2 output data. Using this MCNP core input, power and neutron flux distribution inside the reactor core can be established. The MCNP core criticality calculation is used to determine the neutron fixed source for the MCNP ex-core model. The developed MCNP core model was verified and validated by comparing calculated power densities to CORD-2 results and in-core detector measurements [8]. To accelerate calculations outside the reactor core, weight windows generated using hybrid code ADVANTG [3] are used.

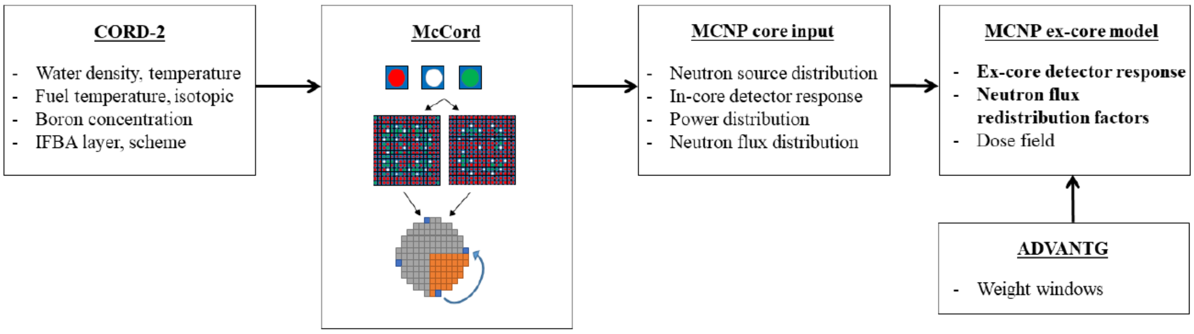

Figure 3: Calculation procedure scheme to obtain ex-core detector response.

4 RESULTS

The aim of the paper is to study the effect of possible detector and core barrel movement during an earthquake on its response.

4.1 Neutron Flux at PRNI and IRNI Positions

Neutron flux at PRNI and IRNI positions was calculated within the active part of the detector and averaged over all channels. Results are presented in Table 1. It can be observed that there are no significant differences between BOC and EOC.

It can be observed that total neutron flux at IRNI is higher than at PRNI position; this is due to different axial positions of detectors. IRNI are positioned approximately at the middle of the active core height, while the PRNI cover almost the entire active core height. The average value of total neutron flux through the whole axial height is lower than the average value of total neutron flux near the core midplane.

The smaller difference between total and thermal neutron flux for IRNI, compared to PRNI, is due to the polyethylene cover, which slows fast neutrons to thermal energies.

Table 1: Total and thermal neutron flux at detector positions.

Detector	ϕ_{tot} [n/cm^{2}s]	ϕ_{th} [n/cm^{2}s]
BOL		
PRNI	2.3×10^{10} (1 $\pm$ 0.04 %)	4.8×10^{9} (1 $\pm$ 0.06 %)
IRNI	3.1×10^{10} (1 $\pm$ 0.07 %)	2.2×10^{10} (1 $\pm$ 0.08 %)
EOL		
PRNI	2.4×10^{10} (1 $\pm$ 0.04 %)	5.1×10^{9} (1 $\pm$ 0.06 %)
IRNI	3.2×10^{10} (1 $\pm$ 0.07 %)	2.3×10^{10} (1 $\pm$ 0.08 %)

In addition, neutron flux at PRNI and IRNI positions was calculated in 100 energy groups. Results are presented in Figure 4. Neutron flux at IRNI is more thermalised, compared to PRNI, due to the presence of polyethylene cover.

Furthermore, total and thermal neutron flux profile was calculated at PRNI and IRNI locations in 2 cm $\times$ 2 cm bins covering the active detector height. In Figure 5 the grid used in calculations is presented. On contrary to the calculations presented above, detectors were not explicitly modelled when studying neutron flux profile on a grid, since we are interested in relative flux changes only.

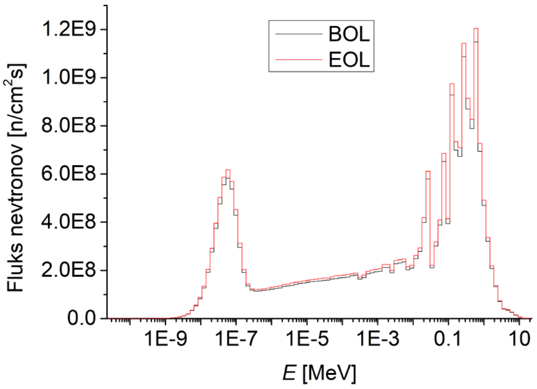

(a) PRNI.

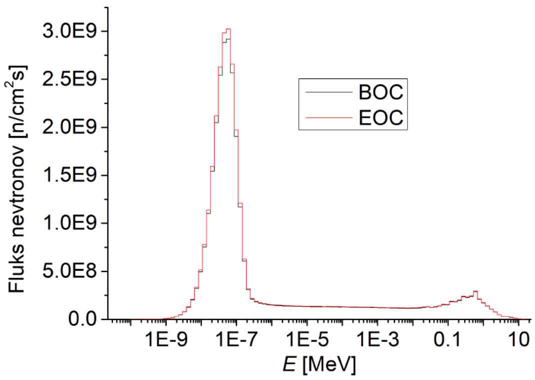

(b) IRNI.

Figure 4: Neutron flux inside active detector region in 100 equidistant energy groups in logarithmic scale.

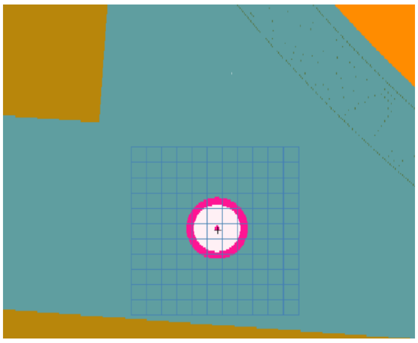

(a) PRNI.

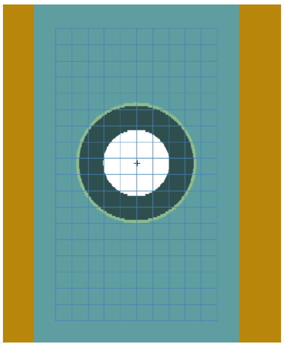

(b) IRNI.

Figure 5: Schematic view of computational grid with presented reference detector position.

Calculated thermal and total neutron flux on a grid for EOC state for IRNI is presented in Figure 6 and for PRNI in Figure 7.

When studying the PRNI the thermal neutron flux has to be observed, while for IRNI the total neutron flux needs to be observed. The calculations of total and thermal neutron flux at IRNI position differ compared to previous calculations, because the detectors were not explicitly modelled and polyethylene cover was not present in the calculations. For calculations performed on a grid, the averaging over different channels was not performed and only SW PRNI and N IRNI detectors were studied. Results presented on a grid can slightly deviate from the results with explicitly modelled detectors (where average over all channels is performed), due to the core and fixed neutron source asymmetry.

4.2 Effect of Ex-core Detector Position

The effect of PRNI and IRNI movement on its response was studied. The explicitly modelled detectors were moved for 5 cm in radial, axial and azimuthal direction and the deviation in detector response was studied. The statistical uncertainty for PRNI ϕ_{tot} is $1\sigma < 0.05$ % and for ϕ_{th} is $1\sigma < 0.06$ %. The statistical uncertainty for IRNI ϕ_{tot} is $1\sigma < 0.08$ % and for ϕ_{th} is $1\sigma < 0.09$ %. Results for EOC are presented in Table 2. It can be observed that total neutron flux decreases when the detector is moved further away from the core and increases when it is moved closer to the reactor core. Similarly can also be observed for thermal neutron flux

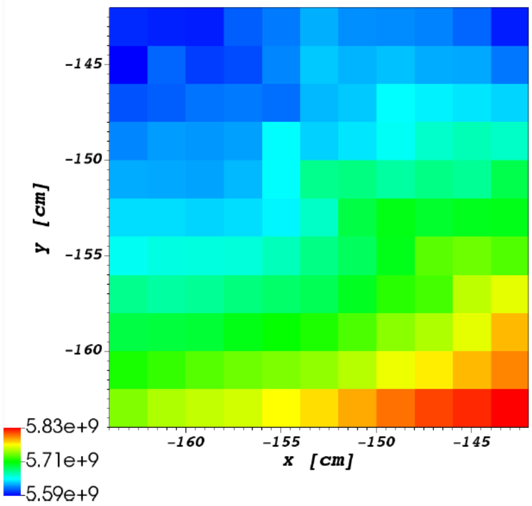

(a) Thermal neutron flux.

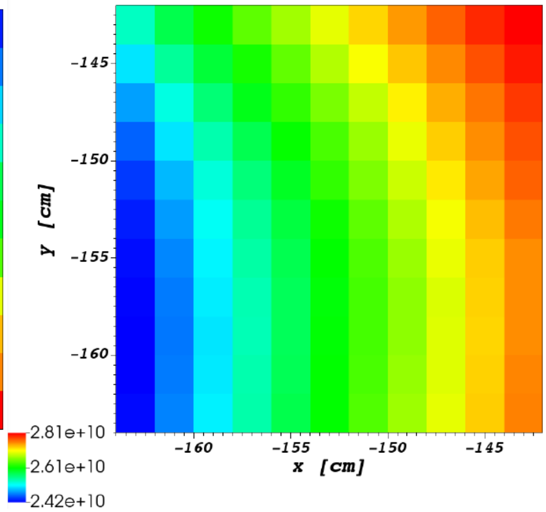

(b) Total neutron flux.

Figure 6: Neutron flux profile for PRNI for EOC core state in n/cm^{2}s.

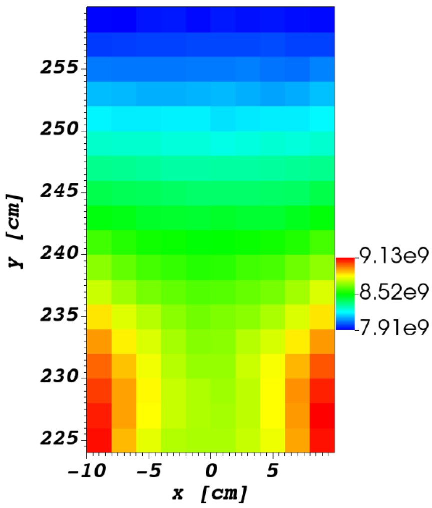

(a) Thermal neutron flux.

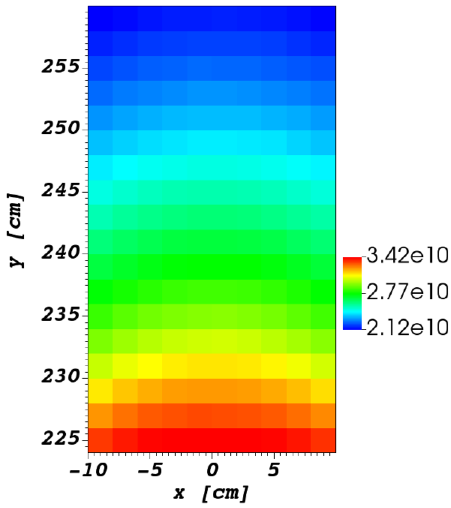

(b) Total neutron flux.

Figure 7: Neutron flux profile for IRNI for EOC core state in n/cm^{2}s.

for IRNI detector. However, thermal neutron flux at PRNI increases when detector is moved further away from the core and decreases when it is moved closer. This can be explained with scattering of neutrons on the concrete surrounding the detector.

It can be concluded that the response of PRNI detector is not highly sensitive to its position. Axial, radial and azimuthal gradients of thermal neutron flux are < 0.2 %/cm, which is within the statistical uncertainty. It can be concluded that the mechanical movement of PRNI detectors during an earthquake can not be the reason for observed deviations in their signal.

Analysing the results for IRNI, it can be observed that radial movement of 5 cm leads to 8 % - 9 % change in the detector response, which is equal to gradient of $\sim$ 1.57 %/cm - 1.95 %/cm. It can be concluded that the deviations in IRNI signal during an earthquake could be significant enough to cause the reactor to shut down automatically. However, the mechanical movement of detectors does not explain the fluctuations in PRNI signal.

Table 2: Deviation in total (ϕ_{tot}) and thermal (ϕ_{th}) neutron flux and their gradient, where z represents movement in axial, r in radial and α in azimuthal direction.

Detector	$\Delta\phi_{tot}$ [%]	Gradient ϕ_{tot} [%/cm]	$\Delta\phi_{th}$ [%]	Gradient ϕ_{th} [%/cm]
PRNI				
z + 5 cm	-0.23	-0.05	-0.19	-0.04
r + 5 cm	-2.90	-0.58	-0.04	-0.01
r - 5 cm	3.03	0.61	0.20	0.04
α + 5 cm	-1.05	-0.21	-0.77	-0.15
α - 5 cm	0.85	0.17	2.16	0.43
IRNI				
z + 5 cm	-0.20	-0.04	-0.21	-0.04
r + 5 cm	-7.87	-1.57	-7.28	-1.46
r - 5 cm	9.04	1.81	8.33	1.67
α + 5 cm	-2.72	-0.54	-2.42	-0.48
α - 5 cm	-2.47	-0.49	-2.16	-0.43

4.3 Effect of Core Barrel Movement

The effect of core barrel movement in radial direction for EOC core state on PRNI and IRNI response was analysed. In calculations, detectors were explicitly modelled and neutron flux was calculated within the active detector volume. To asses the linearity of the effect the core barrel was moved for 2 mm, 5 mm, 7.5 mm and 10 mm in the radial direction, closer to the neutron detector. Results are presented in Figure 8. It can be observed that the deviation from linearity is within statistical uncertainty. The relative deviation in PRNI response with core barrel radial movement closer to the detector leads to a gradient of (1.83 $\pm$ 0.02) %/mm and for IRNI detector (1.97 $\pm$ 0.02) %/mm. If core barrel was moved for 5 mm closer to neutron detectors, it would lead to $\sim$9 % deviation in PRNI response and to $\sim$10 % deviation in IRNI response. It can be concluded that the core barrel movement has a significant effect on detector signal and could be one of the reasons for observed fluctuations in detector signal during an earthquake.

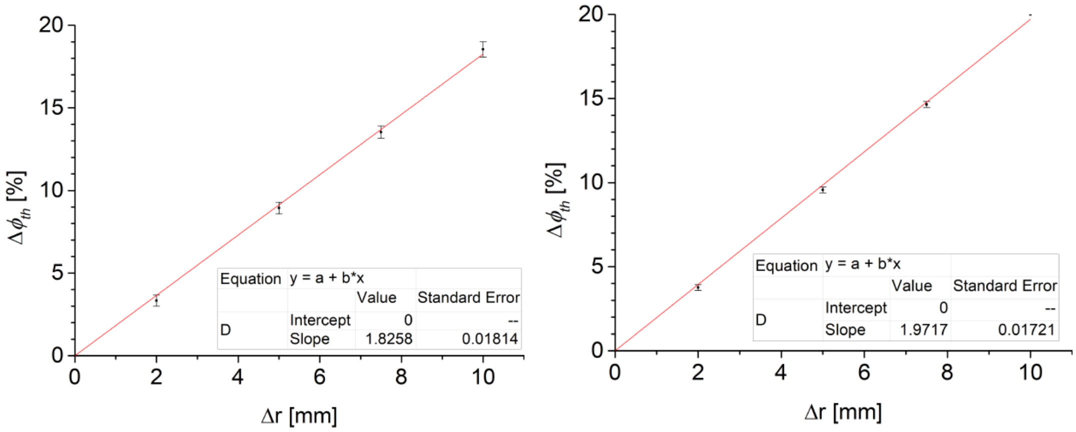

(a) PRNI. (b) IRNI.

Figure 8: Deviation in thermal neutron flux for EOC state due to core barrel radial movement.

5 CONCLUSION

This paper present the analysis of the effect of Krško NPP ex-core detector position on their response. It was found that mechanical movement of detectors has negligible effect on PRNI response, however the effect on IRNI was noticeable and was up to 8 % in radial direction and $\sim$2 % in azimuthal direction. The analysis continued with the evaluation of the effect of core barrel movement on the ex-core detector response. It was found out that 5 mm radial movement of core barrel leads to 9 % and 10 % deviation for PRNI and IRNI, respectively. This leads to the conclusion that core barrel movement could be one of the reasons for observed fluctuations in ex-core detector signal during an earthquake.

ACKNOWLEDGEMENTS

We acknowledge that this work is supported by the project "Ocena vpliva pozicije zunajsrediščnih detektorjev moči na njihov signal" (SP-ES1391) by the Krško Nuclear Power Plant.

REFERENCES

[1] J.T. Goorley, et al., "Initial MCNP6 Release Overview - MCNP6 version 1.0", LA-UR-13-22934, 2013.

[2] D.A.Brown, et al., "ENDF/B-VIII.0: The 8th major release of the nuclear reaction data library with CIELO-project cross sections, new standards and thermal scattering data", Nucl. Data Sheets 148(2018)1.

[3] S. W. Mosher, et. al, "ADVANTG An Automated Variance Reduction Parameter Generator", August 2015.

[4] K. Ambrožič, et al., "Characterisation of Neutron Fields in the TRIGA Irradiation Facilities Inside and Outside the Biological Shield", In: Proceedings of 26th International Conference Nuclear Energy for New Europe, Bled, Slovenia, 2017.

[5] T. Goričanec, et al., "Sensitivity analysis of ex-core detector response using different neutron sources in a typical PWR using Monte Carlo methods", International Conference on Radiation Shielding 2020, Seattle, WA, USA, September 2020 (postponed).

[6] T. Goričanec, et al., "Effect of Nuclear Data Libraries on PWR Ex-core Detector Response", In: Proceedings of 29th International Conference Nuclear Energy for New Europe, portorož, Slovenia, 2020.

[7] M. Kromar, A. Trkov, "Nuclear Design Calculations of the NPP Krško Core", Journal of Energy Technology, Vol. 2, pp. 41-50, November 2009.

[8] T. Goričanec, et al., "Applicability of the Krko Nuclear Power Plant Core Monte Carlo model for the determination of the neutron source term", accepted for publication in Nuclear Engineering and Technology, 2021, https://doi.org/10.1016/j.net.2021.05.022.